ACS APPLIED MATERIALS & INTERFACES

Letter

www.acsami.org

3D Cross-Linked Nanoweb Architecture of Binder-Free TiO_2 Electrodes for Lithium Ion Batteries

Sangkyu Lee,[†,‡] Jaehwan Ha,[†,‡] Junghyun Choi,[§] Taeseup Song,[†] Jung Woo Lee,[§] and Ungyu Paik*[,§]

[†]Division of Materials Science Engineering and [§]WCU Department of Energy Engineering, Hanyang University, Seoul 133-791, Republic of Korea

Supporting Information

ABSTRACT: The nanoweb structure of TiO_2 anode, cross-linked between electrospun nanofibers, is directly fabricated on the current collector by utilizing the fluidity of low glass transition temperature polymer, poly(vinyl acetate), at room temperature. This characteristic enables us to fabricate the nanoweb structure by direct electrospinning on the current collector, followed by uniaxial pressing. This proposed structure facilitates electron transport through the direct conducting pathways between TiO_2 active materials and current collector as well as provides strong adhesion strength to the current collector without polymeric binders. Consequently, we could achieve stable cycle performance up to 100 cycles and the excellent rate capability of ~60% at high rate charge/discharge condition of 10 *C*.

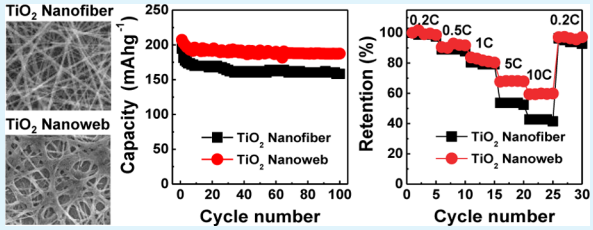

KEYWORDS: *cross-linked, nanoweb, binder-free, electrospinning, titanium oxide (TiO_2), lithium ion battery*

1. INTRODUCTION

Titanium oxide (TiO_2) is an attractive material for lithium ion battery anodes with high safety and stability because Li ions can be inserted into TiO_2 matrix at higher voltage (at least 1.5 V vs. Li/Li^+) than graphite.[1,2] However, its poor electronic conductivity and lithium ion diffusivity lead to the limited electrochemical performance of TiO_2-based lithium ion batteries. In general, to resolve such intrinsic drawbacks of electrode materials, researchers have proposed the use of nanomaterials and their structural design and the application of additives. As regards nanomaterials, they provide short diffusion length for lithium ions as well as high contact area of electrolyte.[3−5] Among various types of the nanostructures, one-dimensional (1D) structures such as nanorods, nanowires, nanotubes, and nanofibers are considered as the promising nanostructures for high performance electrodes.[6−8] This is in part due to their nature of a long 1D structure with a nanoscale diameter, enabling faster electron transport without retardation at the interfaces while maintaining the advantages of nanomaterials with shorter diffusion length of Li ion and higher contact area facing with the electrolyte solution. The electrodes prepared with such 1D nanostructured materials are also fabricated by the same procedure of fabricating conventional electrode for lithium ion batteries that is a serial process of mixing of active materials with conducting additive and polymeric binder, followed by casting on the current collector. However, agglomeration phenomenon can occur during the mixing process, leading to the segregated components and consequently the formation of interrupted, noncontinuous pathways for Li ions and electrons. For example, the segregation of binders can cause severe problems like blocking the conducting pathways because the polymeric binders are electrically insulating.[9,10] Further, the electrochemical inactivity of conducting additive and polymeric binder decreases the specific mass capacity of the whole energy storage system.

To overcome the aforementioned issues, an alternative approach to construct a nanostructure of wholly active materials that is directly connected to the current collector without conducting additives and polymeric binders was recently suggested.[11−13] Recently, we also proposed sol−gel nanoglues consisting of active material to adhere the electrospun active materials on the current collector.[14] The nanofiber electrode strengthened with sol−gel nanoglues exhibited excellent cycle performance and Coulombic efficiency, which is attributed to the intimate contact between individual nanofibers as well as nanofibers and current collector. Despite achieving excellent electrochemical performance, there are some disadvantages of complexity of two step fabrication processing and requirement of large amounts of sol−gel nanoglues.

Here, we demonstrate a facile single annealing step preparation of binder-free TiO_2 nanofiber-based electrode with a unique structure of cross-linked nanostructure of TiO_2 nanofibers for use in lithium ion battery anodes. A mixture of TiO_2 precursor and a low glass transition temperature polymer is utilized to prepare TiO_2 nanofibers. TiO_2 nanofibers are directly electrospun on the current collector, followed by uniaxial pressing at room temperature. Low glass transition temperature polymer of poly(vinyl acetate) (PVAc) has a certain level of freedom of movements near the room

Received: September 19, 2013
Accepted: November 11, 2013
Published: November 11, 2013

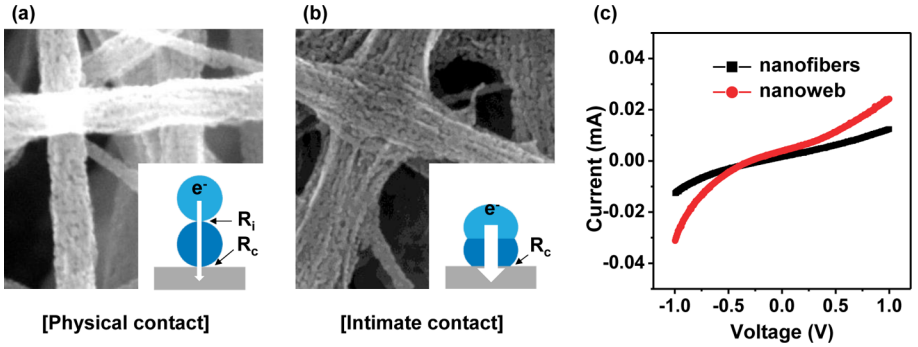

Figure 1. Schematic illustration of electron conduction mechanism in (a) TiO_2 nanofibers and (b) TiO_2 nanoweb anodes, and (c) the current–voltage (I–V) characteristics of both nanostructures.

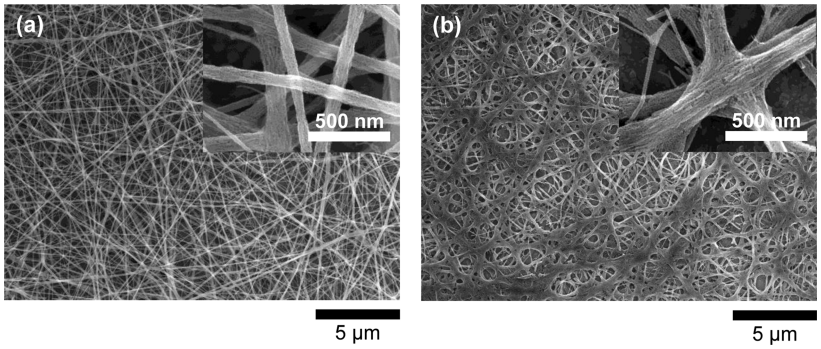

Figure 2. SEM images of (a) TiO_2 nanofibers and (b) TiO_2 nanoweb.

temperature, enabling the transport of TiO_2 precursor along with the polymer during the uniaxial pressing, and consequently leading to the cross-linked nanostructure of TiO_2 nanofibers. This unique structure increases adhesion strength of nanofibers on the current collector without the use of polymeric binders and improves electrical contact properties between individual nanofibers as well as nanofibers and current collector. We refer to this cross-linked unique structure as "nanoweb".

2. RESULTS AND DISCUSSION

3D Cross-Linked Nanoweb Architecture of TiO_2 Electrode. Figure 1 illustrates the advantages of our unique nanoweb structure. In the case of general direct electrospinning (Figure 1a), the underlying layers of nanofibers are surmounted by the upper layers of nanofibers, producing physical and weak connection between two layers.[14] Two interfacial resistances including the resistance between nanofibers (R_i), and nanofiber/current collector (R_c) co-exist in the electrodes along with the intrinsic resistance of TiO_2. Thus, the influence of the interfacial resistance between the nanofibers (R_i) accumulates with increasing the thickness of nanofiber layers. PVAc, which is employed as a shape forming polymer for TiO_2 nanofibers, has a low glass transition temperature of 28–30 °C,[15] which provides low level of fluidity to the nanofibers at room temperature. TiO_2 precursor can be transported along with the movement of PVAc during the uniaxial pressing, leading to the formation of junction between the underlying and upper layers of nanofibers (Figure 1b and Figure S1 in the Supporting Information). On the other hand, poly(methyl methacrylate) with high glass transition temperature of 105 °C does not lead to the formation of cross-linked structure (Figure S2 in the Supporting Information.) The junction guarantees intimate contact, therefore the interfacial resistance between the nanofibers can be ignored. To verify this concept, we measured the current–voltage (I–V) characteristics for both structures and the results are shown in Figure 1c. Higher current flows through the TiO_2 nanoweb structure, which is evidently indicative that the nanoweb structure is favorable for the electron transport compared to the nanofiber structure. On the basis of this concept, it can be expected that electrons are effectively transferred through the TiO_2 nanoweb anode compared to the TiO_2 nanofiber anode, leading to the high performance lithium ion batteries.

Figure 2 shows the scanning electron microscopy (SEM) images of TiO_2 nanofibers and nanoweb. After annealing for the removal of polymeric phase, TiO_2 nanofibers exist separately and their diameter is ~100 nm (Figure 2a). In the case of TiO_2 nanoweb (Figure 2b), cross-linking at the nanofiber junctions can be clearly observed. Both TiO_2 nanostructures exhibit anatase phase (see Figure S3 in the Supporting Information). However, a faint trace of rutile phase is also observed at 27.6° in both TiO_2 nanostructures

Galvanostatic charge and discharge cycle tests were performed using TiO_2 nanofibers and nanoweb electrodes in the voltage range of 1–3 V vs. Li/Li^+. Figure 3a compares the first charge/discharge curves for TiO_2 nanofibers and nanoweb electrodes at the current rate of 0.2 C (1 C = 200 mA g^{-1}). TiO_2 nanofibers electrode yields the first charge capacity of 195 $mAhg^{-1}$ and the discharge capacity of 319 $mAhg^{-1}$. On the other hand, TiO_2 nanoweb electrode delivers the first charge capacity of 207 $mAhg^{-1}$ and the discharge capacity of 255 $mAhg^{-1}$. The first Coulombic efficiencies of TiO_2 nanofibers and nanoweb electrodes are 61.1 and 81.3%, respectively. There are two clear plateaus at ~1.91 and 1.76 V in the charge and discharge curves, respectively, which corresponds to the phase transition between anatase TiO_2 and lithiated TiO_2.[16] This

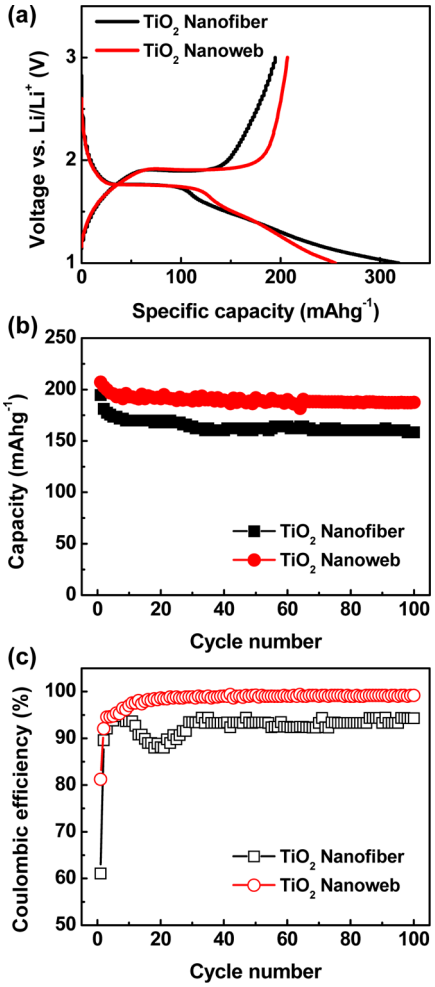

Figure 3. Electrochemical properties of TiO_2 nanofibers and nanoweb electrodes. (a) First charge–discharge voltage profiles at 0.2 *C*, (b) cycling performance, and (c) Coulombic efficiency.

result clearly indicates the formation of electrochemically stable TiO_2 phases in both TiO_2 nanofibers and nanoweb. The variations of the charge capacity of TiO_2 electrodes are plotted as a function of cycle number in Figure 3b. The charge capacity of TiO_2 nanofibers electrode severely decreases during the initial 5 cycles and then slightly decreases. After 100 cycles, the electrode retains the charge capacity of 158 $mAhg^{-1}$, which corresponds to 81.4% of initial charge capacity. On the contrary, TiO_2 nanoweb electrode delivers the charge capacity of 188 $mAhg^{-1}$ after 100 cycles, indicating that 90.5% of initial charge capacity retains. The Coulombic efficiencies of both electrodes as a function of cycle are also compared as shown in Figure 3c. TiO_2 nanoweb electrode approaches the Coulombic efficiency of >99%, whereas the efficiency of TiO_2 nanofibers shows severe fluctuation. The instability in the Coulombic efficiency for TiO_2 nanofibers originates from the weak adhesion of nanofibers on current collector.[14]

Such structural benefits of the nanoweb structure can be observed in the rate capability of TiO_2 nanoweb electrode. The rate capability was tested with increasing current density from 0.2 to 10 *C*. The rate capability was calculated by dividing the capacity at a given current density by the capacity at the current rate of 0.2 *C* and the results are shown in Figure 4. TiO_2 nanofibers electrode exhibits the capacity retention of ~40% at the current rate of 10 *C*, which is higher than that of reported

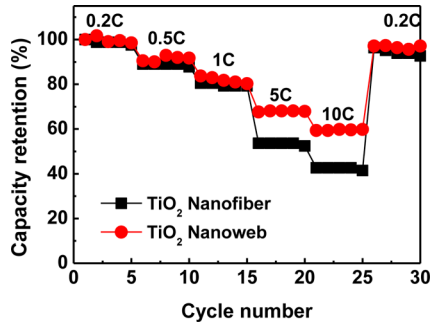

Figure 4. Rate capabilities of TiO_2 nanofibers and nanoweb electrodes.

values for conventional TiO_2 electrodes fabricated with conducting additives and polymeric binders.[6,17−21] It can be explained by the fact that the presence of these components can affect the electrochemical reactions between Li ions and electrode materials. This result clearly shows that the formation of direct conducting pathways between electrode and current collector can be an effective approach to improve the electrochemical performance of electrode. In addition, we verify that rate capability can be further improved by applying the nanoweb structure. The rate capability of TiO_2 nanoweb electrode is ~60% at the current density of 10 *C*, which exceeds that of the TiO_2 nanofibers electrode. It indicates that the formation of nanoweb structure is much more favorable to fabricate high rate lithium ion batteries than as-received nanofiber structure.

To interpret the improved electrochemical performance of TiO_2 nanoweb electrode, we utilized electrochemical impedance spectroscopy. The results are plotted as a Nyquist plot (Figure 5). The Nyquist plot consists of a semicircle at high-to-

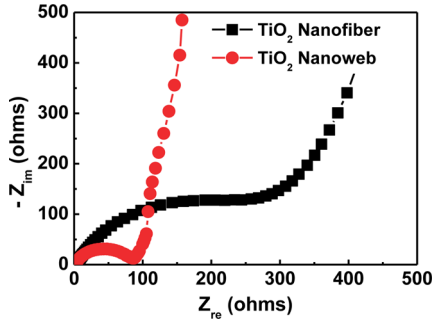

Figure 5. Nyquist plots of TiO_2 nanofibers and nanoweb electrodes.

medium frequencies followed by a straight line in the low frequency region. In the semicircle, the *x*-intercept corresponds to the Ohmic resistance of bulk cell including electrolyte, separator, and electrode. The Ohmic resistance of TiO_2 nanofibers and nanoweb are 3.3 and 2.5 Ω, respectively. This difference can originate from the unique structure of TiO_2 nanoweb since other components of both the TiO_2 electrodes are identical. The extrapolated right most end of the semicircle, indicating the resistance at the medium frequency (polarization resistance), relates to the electrolyte transport resistance in the solid electrolyte interface and the charge transfer resistance of Li^+ to the TiO_2 electrode. TiO_2 nanoweb electrode clearly shows low polarization resistance (< 90 Ω) than that of TiO_2 nanofibers electrode. This decreased polarization resistance, which is observed in the nanoweb electrode, is attributed to the merged intersects that provides well connected conducting

dx.doi.org/10.1021/am404082h | *ACS Appl. Mater. Interfaces* 2013, 5, 11525−11529

pathways. Therefore, this Nyquist plot clearly explains the mechanism for the improved electrochemical performance of TiO_2 nanoweb electrode.

Delamination Issue of Directly Electrospun Nanofibers. Additionally, the proposed methodology to fabricate nanoweb structure solves a chronic delamination issue of the direct electrospinning process. Figure S4 in the Supporting Information describes the delamination of TiO_2 nanofibers, which were directly electrospun on the current collector and then annealed. At low loading level, the electrospun TiO_2 nanofibers remain adhered on the current collector after annealing. However, partial delamination occurs in the TiO_2 nanofibers with higher loading level of 0.0557 mg/cm^2. Further increase in the loading level leads to complete delamination, leaving a trace of nanofibers. Thus, we fabricated TiO_2 nanofibers electrode below this limitation. A serial process of direct electrospinning, uniaxial pressing, and annealing produces TiO_2 nanoweb structure on the current collector. Contrary to the TiO_2 nanofibers, TiO_2 nanoweb strongly adheres on the current collector, enabling higher loading of electrode materials without delamination. Therefore, the proposed methodology is effective to increase the areal capacity of nanostructured material-based electrode. The areal capacity of TiO_2 nanoweb electrode can exceed that of our recent TiO_2 nanotube electrode directly grown on the current collector.[7] Table S1 in the Supporting Information compares the areal density of TiO_2 nanofibers and TiO_2 nanoweb electrodes. Many efforts have been made to prevent the delamination of nanofibers during annealing process. Hot pressing[15,22,23] and solvent treatment[24] are proposed for this reason. However, the original nanostructure can be severely deformed during these processes. The deformation of nanostructure can decrease surface area, leading to the deterioration of electrochemical performance of nanostructure-based electrode. On the contrary, uniaxial pressing method proposed here is conducted at room temperature, which avoids the massive deformation of TiO_2 nanofibers. This methodology utilizes the fluidity of a polymer with low glass transition temperature; therefore, it can be applied to a variety of nanomaterials without the severe deformation.

3. CONCLUSIONS

In summary, we report a methodology to fabricate high performance electrodes for electrochemical energy storage devices without conducting additives and polymeric binders. This approach utilizes electrospun nanofibers which were directly electrospun on the current collector and adapts a uniaxial pressing to provide superior mechanical and electrical contact properties between nanofibers and current collector as well as between nanofibers. The resulting nanostructure is referred to as "nanoweb". This methodology is applied to fabricate TiO_2 nanofiber electrodes for Li ion batteries. The resulting TiO_2 nanoweb anodes exhibit stable cycling performance of 90.5% up to 100 cycles with high initial Coulombic efficiency of 81.3% and show the excellent capacity retention of ~60% at 10 *C*. The direct contact of TiO_2 nanofibers on the current collector and the cross-linking of the stacked nanofibers at the intersecting points provide a highly effective electron conducting pathways in the entire electrode system, which results in the stable cycling performance and the formidable high rate capacity retention. From the point of the improvement, this work provides an alternative methodology of fabricating high performance lithium ion batteries. Moreover, we expect that it can be adapted to prepare electrodes of other energy storage devices as well as other Li ion anodes showing poor rate capability.

■ ASSOCIATED CONTENT

Ⓢ Supporting Information

Experimental procedures for preparing TiO_2 nanofibers and nanoweb structure, fabricating lithium ion batteries, characterizing the material properties of TiO_2 nanofibers and nanoweb structure, and evaluating the electrochemical performance of the electrodes. Also, the cross-sectional image of TiO_2 nanoweb structure, SEM image of TiO_2 nanofiber prepared with a mixture of TiO_2 precursor and PMMA solution, calculated areal capacities, XRD patterns of both nanostructures, and photographs to describing the delamination phenomenon of the electrospun nanofibers during the annealing process. This material is available free of charge via the Internet at http://pubs.acs.org.

■ AUTHOR INFORMATION

Corresponding Author

*E-mail: upaik@hanyang.ac.kr. Tel: +82-2-2220-0502. Fax: +82-2-2281-0508.

Author Contributions

‡Authors S.L. and J.H. contributed equally to this work

Notes

The authors declare no competing financial interest.

■ ACKNOWLEDGMENTS

This work was supported by the Global Research Laboratory (GRL) Program (K20704000003TA050000310) through the National Research Foundation of Korea (KRF) funded by the Ministry of Science, ICT (Information and Communication Technologies) and Future Planning, the International Cooperation program of the Korea Institute of Energy Technology Evaluation and Planning (KETEP) grant funded by the Korea government of Ministry of Trade, Industry & Energy (2011T100100369).

■ REFERENCES

(1) Wang, J.; Bai, Y.; Wu, M.; Yin, J.; Zhang, W. F. *J. Power Sources* **2009**, *191*, 614−618.
(2) Pfanzelt, M.; Kubiak, P.; Fleischhammer, M.; Wohlfahrt-Mehrens, M. *J. Power Sources* **2011**, *196*, 6815−6821.
(3) Arico, A. S.; Bruce, P.; Scrosati, B.; Tarascon, J. M.; Van Schalkwijk, W. *Nat. Mater.* **2005**, *4*, 366−377.
(4) Wang, J.; Zhou, Y.; Hu, Y.; O'Hayre, R.; Shao, Z. *J. Phys. Chem. C* **2011**, *115*, 2529−2536.
(5) Zakharova, G. S.; Jähne, C.; Popa, A.; Täschner, C.; Gemming, T.; Leonhardt, A.; Büchner, B.; Klingeler, R. *J. Phys. Chem. C* **2012**, *116*, 8714−8720.
(6) Han, H.; Song, T.; Bae, J. Y.; Nazar, L. F.; Kim, H.; Paik, U. *Energy Environ. Sci* **2011**, *4*, 4532−4536.
(7) Han, H.; Song, T.; Lee, E.-K.; Devadoss, A.; Jeon, Y.; Ha, J.; Chung, Y.-C.; Choi, Y.-M.; Jung, Y.-G.; Paik, U. *ACS Nano* **2012**, *6*, 8308−8315.
(8) Wu, H. B.; Chen, J. S.; Hng, H. H.; Wen Lou, X. *Nanoscale* **2012**, *4*, 2526−2542.
(9) Liu, G.; Zheng, H.; Simens, A. S.; Minor, A. M.; Song, X.; Battaglia, V. S. *J. Electrochem. Soc.* **2007**, *154*, A1129−A1134.
(10) Liu, G.; Zheng, H.; Kim, S.; Deng, Y.; Minor, A. M.; Song, X.; Battaglia, V. S. *J. Electrochem. Soc.* **2008**, *155*, A887−A892.
(11) Jang, H. D.; Kim, S. K.; Chang, H.; Roh, K.-M.; Choi, J.-W.; Huang, J. *Biosens. Bioelectron.* **2012**, *38*, 184−188.

(12) Zhao, B.; Cai, R.; Jiang, S.; Sha, Y.; Shao, Z. *Electrochim. Acta* **2012**, *85*, 636−643.
(13) Zhao, B.; Shao, Z. *J. Phys. Chem. C* **2012**, *116*, 17440−17447.
(14) Choi, J.; Lee, S.; Ha, J.; Song, T.; Paik, U. *Nanoscale* **2013**, *5*, 3230−3234.
(15) Kim, I. D.; Rothschild, A.; Lee, B. H.; Kim, D. Y.; Jo, S. M.; Tuller, H. L. *Nano Lett.* **2006**, *6*, 2009−2013.
(16) Chen, J. S.; Tan, Y. L.; Li, C. M.; Cheah, Y. L.; Luan, D.; Madhavi, S.; Boey, F. Y. C.; Archer, L. A.; Lou, X. W. *J. Am. Chem. Soc.* **2010**, *132*, 6124−6130.
(17) Wang, D.; Choi, D.; Li, J.; Yang, Z.; Nie, Z.; Kou, R.; Hu, D.; Wang, C.; Saraf, L. V.; Zhang, J.; Aksay, I. A.; Liu, J. *ACS Nano* **2009**, *3*, 907−914.
(18) Nam, S. H.; Shim, H.-S.; Kim, Y.-S.; Dar, M. A.; Kim, J. G.; Kim, W. B. *ACS Appl. Mater. Interfaces* **2010**, *2*, 2046−2052.
(19) Luo, W.; Hu, X.; Sun, Y.; Huang, Y. *J. Mater. Chem.* **2012**, *22*, 4910−4915.
(20) Yang, Z.; Du, G.; Meng, Q.; Guo, Z.; Yu, X.; Chen, Z.; Guo, T.; Zeng, R. *J. Mater. Chem.* **2012**, *22*, 5848−5854.
(21) Zhu, P.; Wu, Y.; Reddy, M. V.; Sreekumaran Nair, A.; Chowdari, B. V. R.; Ramakrishna, S. *RSC Adv.* **2012**, *2*, 531−537.
(22) Landau, O.; Rothschild, A.; Zussman, E. *Chem. Mater.* **2009**, *21*, 9−11.
(23) Hwang, D.; Jo, S. M.; Kim, D. Y.; Armel, V.; MacFarlane, D. R.; Jang, S.-Y. *ACS Appl. Mater. Interfaces* **2011**, *3*, 1521−1527.
(24) Onozuka, K.; Ding, B.; Tsuge, Y.; Naka, T.; Yamazaki, M.; Sugi, S.; Ohno, S.; Yoshikawa, M.; Shiratori, S. *Nanotechnology* **2006**, *17*, 1026−1031.